Driven quantum dot coupled to a fractional quantum Hall edge

Glenn Wagner [●],[1] Dung X. Nguyen,[1] Dmitry L. Kovrizhin,[1,2] and Steven H. Simon[1]

[1]*Rudolf Peierls Centre for Theoretical Physics, Parks Road, Oxford, OX1 3PU, United Kingdom*
[2]*NRC Kurchatov Institute, 1 Kurchatov Square, 123182, Moscow, Russia*

We study a model of a quantum dot coupled to a quantum Hall edge of the Laughlin state, taking into account short-range interactions between the dot and the edge. This system has been studied experimentally in electron quantum optics in the context of single particle sources. We consider driving the dot out of equilibrium by a time-dependent bias voltage. We calculate the resulting current on the edge by applying the Kubo formula to the bosonized Hamiltonian. The Hamiltonian of this system can also be mapped to the spin-boson model and, in this picture, the current can be perturbatively calculated using the noninteracting blip approximation. We show that both methods of solution are in fact equivalent. We present numerics demonstrating that the perturbative approaches capture the essential physics at early times, although they fail to capture the charge quantization (or lack thereof) in the current pulses integrated over long times.

I. INTRODUCTION

Electron quantum optics (EQO) is a field devoted to the study and manipulation of single electron excitations. A promising platform for EQO experiments has proven to be the edge states of the fractional quantum Hall effect (FQHE) [1]: Since the edge states are chiral, there is no possibility of backscattering. An important ingredient in any EQO experiment is a single-electron source and in the present paper we study a model of such a device. The model is comprised of a chiral FQHE Laughlin edge state, which we model as a Luttinger liquid. The edge is coupled to a quantum dot via a quantum point contact (QPC). By applying a time-dependent gate voltage to the dot, one is able to obtain current pulses on the edge. The setup is shown in Fig. 1. In a recent paper [2], the present authors highlighted the effect of interactions in this setup, resulting in a nonquantized charge in the pulses on the edge. In this paper, we use a different set of techniques to study the same problem, which allows us to extend our results to different regimes.

For these purposes, we focus on the mapping, originally proposed by Furusaki and Matveev [3], between the spin-boson model and the chiral Luttinger liquid coupled to a single energy level. The spin-boson model—which describes a spin interacting with a bosonic heat bath—is an important archetype of a quantum dissipative system [4–11]. Among other applications, it has been used to describe decoherence of qubits in quantum information science [12,13]. In this paper, we present the details of the mapping between the spin-boson model and a FQHE edge state coupled to a quantum dot (QD) [3].

This correspondence proves to be useful for our purposes, since many analytical and numerical techniques have been developed for the spin-boson model, including the noninteracting blip approximation (NIBA) [14], generalized master equation (GME) [15], stochastic Schrödinger equation description [6], Bethe-ansatz [16] solution, numerical renormal-

ization group [10,17], exact mapping between the spin-boson and the Kondo model [3] and, most recently, tensor network methods [18,19]. Conversely, it is possible to envisage the QD setup as a quantum simulator for the spin-boson model.

For pedagogical purposes and as a consistency check of the mapping from Luttinger liquid to spin-boson model, we use perturbation theory to calculate the current downstream from the dot within both original and dual descriptions. In the bosonization language, the current is obtained from the Green's functions for the vertex operators, while in the spin-boson language we apply the perturbative solution described in Ref. [14], the so-called NIBA. Using perturbation theory to the second order in the tunneling between the dot and the edge we show that both pictures yield identical results. We benchmark this perturbative solution against nonperturbative schemes that are valid at special points in the parameter range of the Hamiltonian. For example, in the case where the FQHE edge is in the integer quantum Hall regime, the problem can be solved exactly. Although this solution has been obtained previously, we present a simpler derivation of the integer quantum Hall result. The perturbative solution is shown to be a very good approximation to that solution at early times.

There have been numerous theoretical works [11,20–36] on single-particle electron emitters. However, in contrast to the previous body of work, here we focus on the nonequilibrium setting, where the energy level of the QD varies with time under applied time-dependent bias voltage. The time evolution of the system in this setup is an interesting problem both from the theoretical and experimental perspective.

Similar setups have also been implemented in recent experiments [37–40]. In particular, in Ref. [37], the QD is driven by a square wave voltage. This experiment studies the edge in the integer quantum Hall regime. Current pulses are detected on the edge downstream from the QD. See also Refs. [1,41,42] for more details of experiments. We hope that the formulas that we derive will be useful for experimentalists when analyzing the measured current pulses. In particular, we
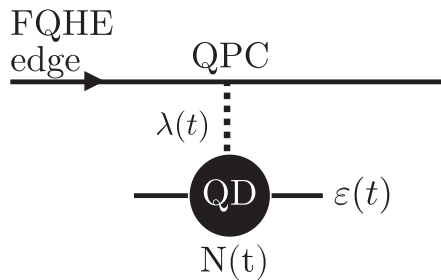
FIG. 1. Schematic model of the experimental setup showing a quantum dot (QD) coupled to an FQHE edge state. The edge is coupled to the dot via a quantum point contact (QPC) at $x = 0$. The gate voltage can be used to tune the tunneling $\lambda(t)$ between the dot and the edge. A single energy level $\varepsilon(t)$ on the quantum dot is controlled via applied bias voltage. We study the occupation number $N(t)$ of the dot over time.

have the central result Eq. (25) for the current on the edge, from which an even simpler analytical expression Eq. (29) can be derived for a particular drive protocol.

The outline of the paper is the following. In Sec. II A, we introduce the model and notations. Section II B presents the mapping between the QD-FQHE model and the spin-boson model, see also Ref. [2]. In Sec. III A, we bosonize the original Hamiltonian and obtain a perturbative solution which is valid at short times. In sSec. III B, we use the NIBA solution to derive the expression for the current, and in Sec. III C we present a comparison between the results obtained using these approaches. Section IV presents numerical results comparing the perturbative solution to two exact solutions valid in certain parameter regimes. In Sec. V, we derive analytical results for the current in a number of physically interesting limits. The exact calculation in the case of integer quantum Hall edge state and further details are presented in the Appendices.

II. THE MODEL AND ITS MAPPING TO THE SPIN-BOSON PROBLEM

A. Model

In this paper, we study a model of a QD or antidot with a single energy level that is coupled to a FQHE edge state. The model is described by the time-dependent Hamiltonian

$$\hat{H}(t) = \hat{H}_0(t) + \hat{H}_{\text{tun}}(t) + \hat{H}_{\text{int}}, \qquad (1)$$

where the terms on the right-hand side correspond to the Hamiltonian of the dot/antidot and the edge ($\hat{H}_0$), the tunneling at the QPC ($\hat{H}_{\text{tun}}$), and the interactions between the dot/antidot and the edge ($\hat{H}_{\text{int}}$), respectively. The Hamiltonian $\hat{H}_0(t)$ describing the dot/antidot and the edge without coupling is given by the following expression:

$$\hat{H}_0(t) = \varepsilon(t)\hat{S}_z + \frac{v}{2}\int \frac{dx}{2\pi}\,(\partial_x\hat{\varphi})^2. \qquad (2)$$

Here the first term on the right-hand side is the energy of a QD/antidot with a single level, and we use operators $\hat{S}^+/\hat{S}^-$ to describe creation/annihilation of a spinless electron or quasielectron on this level. A QD is situated on the outside of the quantum Hall fluid and can only host electrons. If we want to host Laughlin quasiparticles we need to consider

an antidot, which has to be located inside the quantum Hall fluid. Since we want to consider both the cases of electron and quasiparticle tunneling, we need to allow for both the case of a dot and antidot. In the case of a dot, $\hat{S}^+$ creates a electron with charge $q = -e$ (with $e > 0$ being the elementary charge), whereas in the case of an antidot we assume we have quasielectrons tunneling so $\hat{S}^+$ creates a quasielectron with charge $q = -\nu e$. Note that the case of holes or quasiholes is equivalent to electrons or quasielectrons which tunnel in the opposite direction, therefore we do not need to consider this case separately. For conciseness, in the following we will use QD to refer to either a dot or antidot, where it is understood that we are considering a dot when electrons are tunneling and an antidot when quasielectrons are tunneling.

While the spin operators describing the level on the dot satisfy commutation relations which are different to those of electron or quasielectron operators, we show in Appendix B that the associated statistical phase does not enter the results for the current and therefore our spin representation is justified for our purposes. The presence or absence of a particle on the dot is measured by the operator $\hat{N} = \hat{S}_z + 1/2$. The energy level of the dot is a function of time $\varepsilon(t)$ and is controlled by an applied time-dependent bias voltage. In comparison with the previous work [3,21,23,24,26–29], which focused on the case of a constant bias $\varepsilon(t) = \text{const}$, here we study a time-dependent problem.

The second term in Eq. (2) is the bosonized Hamiltonian of an FQHE edge with the length L describing a Laughlin state at filling fraction $\nu = 1/(2n + 1)$ where $n = 0, 1, 2, \ldots$ [43]. The bosonic field can be expanded in its eigenmodes with momentum $k = 2\pi m/L$, $m \in Z$ as follows [44]:

$$\hat{\varphi}(x) = -\sum_{k>0}\sqrt{\frac{2\pi}{kL}}(\hat{b}_k e^{ikx} + \hat{b}_k^\dagger e^{-ikx})e^{-ka/2}, \qquad (3)$$

where a is the short-distance cutoff. The commutation relations of the bosonic operators $\hat{b}_k$ are given by $[\hat{b}_k, \hat{b}_{k'}^\dagger] = \delta_{kk'}$.

The electron and the quasiparticle operators in the bosonization language are vertex operators of the form [43]

$$\hat{\psi}(x) = \frac{1}{\sqrt{2\pi}}\left(\frac{L}{2\pi}\right)^{-\frac{\gamma^2}{2}} : e^{-i\gamma\hat{\varphi}(x)} :, \qquad (4)$$

where $\gamma = 1/\sqrt{\nu}$ or $\gamma = \sqrt{\nu}$ for electrons with charge $-e$ and quasiparticles with charge $-\nu e$ correspondingly, and $: \cdots :$ denotes normal ordering. Note that we have omitted Klein factors since in our problem they do not affect the results for the current, see Appendix B. Using results of Ref. [44], we rewrite the expression for the vertex operators as

$$\hat{\psi}(x) = \frac{1}{\sqrt{2\pi}}a^{-\frac{\gamma^2}{2}}e^{-i\gamma\hat{\varphi}(x)}. \qquad (5)$$

The Hamiltonian describing tunneling of electrons or quasiparticles between the dot and the edge is given by

$$\hat{H}_{\text{tun}}(t) = \lambda(t)\hat{\psi}^\dagger(0)\hat{S}^- + \text{H.c.}, \qquad (6)$$

where the tunneling amplitude $\lambda(t)$ is any time-dependent function. Below we will focus on the the specific case of $\lambda(t) = \lambda\theta(t)$, which corresponds to the situation when the tunneling has been suddenly turned on at $t = 0$. We have also

studied the effects of a gradual switching of the tunneling in the form $\lambda(t) = \lambda \tanh(t/t_s)$, where t_s is some timescale. However, we find that it does not change the qualitative behavior of the current.

We model the Coulomb interactions between the dot and the edge using the following Hamiltonian:

$$\hat{H}_{\text{int}} = -\gamma \frac{g}{2\pi} \partial_x \hat{\varphi}(0) \hat{S}_z, \tag{7}$$

where we used a bosonized form of the charge density operator on the edge $\hat{\rho}(x) = +e\sqrt{\nu} \partial_x \hat{\varphi}/2\pi$, and $g > 0$ is the interaction strength. A detailed discussion of the effects of Coulomb interactions has been presented in our previous work [2], where we showed that the interactions of the form Eq. (7) amount to rescaling of the interaction constant γ such that

$$\tilde{\gamma} = \gamma \left(1 - \frac{g}{2\pi v}\right). \tag{8}$$

By performing the unitary transformation discussed in Sec. II B below, it can be seen that the Coulomb interaction term can be eliminated by this rescaling. The equilibrium occupation of the QD with the Hamiltonian Eq. (1) has been investigated perturbatively in Ref. [3], where the authors found two regimes depending on the strength of $\tilde{\gamma}$. In the weak-tunneling limit, if $\tilde{\gamma} > \sqrt{1/2}$ there is a discontinuity in the occupation number at $\varepsilon = 0$, whereas the latter is continuous for $\tilde{\gamma} < \sqrt{1/2}$.

B. Transformation to the spin-boson problem

In this section, we will study the dynamics of the dot-edge system under the Hamiltonian Eq. (1) using a mapping to the spin-boson model. This mapping is performed using an unitary transformation introduced in Ref. [3]. Let us define a unitary operator $\hat{U}_1 = \exp[-i\gamma\hat{\varphi}(0)\hat{S}_z]$. Using the transformation $\hat{H}_1 = \hat{U}_1^\dagger \hat{H} \hat{U}_1$ and expressing the bosonic fields in terms of their modes via Eq. (3) we obtain

$$\hat{H}_1 = \varepsilon(t)\hat{S}_z + \Delta(t)\hat{S}_x + \sum_{k>0} \omega_k \hat{b}_k^\dagger \hat{b}_k - i\hat{S}_z \sum_{k>0} \eta_k(\hat{b}_k - \hat{b}_k^\dagger), \tag{9}$$

where $\omega_k = vk$ and

$$\Delta(t) = \lambda(t)\sqrt{\frac{2}{\pi}} a^{-\frac{\gamma^2}{2}}, \quad \eta_k = v\tilde{\gamma}\sqrt{\frac{2\pi k}{L}} e^{-ka/2}. \tag{10}$$

The Hamiltonian in Eq. (9) has the standard spin-boson form [5]. The first two terms of Eq. (9) represent a spin-1/2 degree of freedom coupled to a time-dependent magnetic field $\mathbf{B}(t) = \varepsilon(t)\hat{\mathbf{z}} + \Delta(t)\hat{\mathbf{x}}$. The last two terms describe the bosonic bath and the coupling of the spin to the bath, respectively. The spectral function of the bosonic bath is given by the expression

$$J(\omega) = \pi \sum_{k>0} \eta_k^2 \delta(\omega - \omega_k) = 2\pi\alpha\omega\theta(\omega)e^{-a\omega/v}. \tag{11}$$

This spectral function corresponds to the spin-boson model with Ohmic dissipation and with a dimensionless coupling constant $\alpha = \tilde{\gamma}^2/2$. We provide a detailed dictionary of the mapping to the spin-boson model in Table I.

TABLE I. Dictionary of the spin-boson mapping.

QD + FQHE edge	Spin-boson model
Occupation of the QD $\hat{N}$	Spin $\hat{S}_z = \hat{N} - 1/2$
Bosonic operators $\hat{b}_k$	Heat bath bosons $\hat{b}_k$
Vertex exponent $\tilde{\gamma}$	Spin-bath coupling $\alpha = \tilde{\gamma}^2/2$
QD voltage bias $\varepsilon(t)$	Magnetic field $B_z = \varepsilon(t)$
Tunneling $\lambda(t)$	Magnetic field $B_x = \Delta(t)$
IQHE case $\tilde{\gamma} = 1$	Toulouse limit $\alpha = 1/2$

As the next step we refermionize the Hamiltonian Eq. (9) using another unitary transformation $\hat{U}_2 = \exp[i\tilde{\gamma}\hat{\varphi}(0)\hat{S}_z]$ such that $\hat{H}_2 = \hat{U}_2^\dagger \hat{H}_1 \hat{U}_2$ arriving at the Hamiltonian which has the same form as (1) but without the interaction term, and with renormalized tunneling strength

$$\hat{H}_{2,\text{tun}} = \tilde{\lambda}(t)\hat{\tilde{\psi}}^\dagger(0)\hat{S}^- + \text{H.c.}, \tag{12}$$

where the tunneling is given by $\tilde{\lambda}(t) = a^{(\tilde{\gamma}^2 - \gamma^2)/2}\lambda(t)$, and the corresponding $\Delta(t) = \tilde{\lambda}(t)\sqrt{2/\pi}\, a^{-\frac{\tilde{\gamma}^2}{2}}$. After refermionization, the vertex operators assume the following form:

$$\hat{\tilde{\psi}}(x) = \frac{1}{\sqrt{2\pi}} a^{-\frac{\tilde{\gamma}^2}{2}} e^{-i\tilde{\gamma}\hat{\varphi}(x)}. \tag{13}$$

The mapping between the QD system and the spin-boson model is useful, since the latter has been a well-studied problem. It is an archetype of an open quantum system and as such, many numerical techniques have been developed for it. On the other hand, the spin-boson model is difficult to model experimentally. Suggested experiments include trapped ions [45,46] and superconducting circuits [47,48]. The quantum Hall edge setup discussed in this paper is an alternative experimental proposal to study the spin-boson model in the sense of a quantum simulator. Since we know the Hamiltonian for the quantum Hall edge setup, one can perform the experiment to learn about the spin-boson model in regimes that are difficult to access numerically.

III. CALCULATION OF THE CURRENT

In this section, we derive the expression for the time-dependent current using two different perturbative approaches. The first calculation is done in the bosonized Luttinger liquid picture, whereas the second calculation uses well-known results from the spin-boson model. Both give the same answer, which provides a consistency check of the mapping discussed above.

A. Perturbation theory approach for the bosonized Hamiltonian

Here we assume that the QD is weakly coupled (by tunneling) to the FQH edge, and we work in the interaction representation where the tunneling Hamiltonian plays the role of the interactions. The current operator is given by

$$\hat{I}(t) = -\tilde{q}\frac{d\hat{N}}{dt} = -i\tilde{q}[\hat{H}_{2,\text{tun}}(t), \hat{N}(t)], \tag{14}$$

where $\hat{N}(t)$ is the number operator on the QD. We note that, as we have shown in our previous work [2], one has to take

into account the renormalization of the charge

$$\tilde{q} = q\left(1 - \frac{g}{2\pi v}\right). \qquad (15)$$

Intuitively, this renormalization accounts for the fact that the charge density on the edge will be depleted close to the QPC due to Coulomb repulsion. To calculate the expectation of the current to leading order in perturbation theory, we use the Kubo formula

$$I(t) = -i \int_0^t \langle [\hat{I}(t), \hat{H}_{2,\text{tun}}(t')] \rangle \, dt', \qquad (16)$$

where we have assumed that the perturbation switches on at $t = 0$. Using this expression, we arrive at the result for the time-dependent current,

$$\begin{aligned}
I(t) = -\tilde{q} \int_0^t dt' \tilde{\lambda}(t)\tilde{\lambda}(t') \\
\times (e^{i\Omega(t')-i\Omega(t)}[(1-n_a)\Phi(t-t') - n_a\Phi(t'-t)] \\
+ e^{i\Omega(t)-i\Omega(t')}[(1-n_a)\Phi(t'-t) - n_a\Phi(t-t')]),
\end{aligned} \qquad (17)$$

where we defined $\Omega(t) = \int_0^t ds \, \varepsilon(s)$ and $n_a = \langle \hat{N}(0) \rangle$ is the initial occupation of the QD. The correlation function $\Phi(\tau) = \langle \hat{\tilde{\psi}}(0, \tau) \hat{\tilde{\psi}}^\dagger(0, 0) \rangle$ is given by the expression

$$\Phi(\tau) = \frac{1}{2\pi} [iv\tau_B \sinh(\tau/\tau_B - ia/(v\tau_B))]^{-\tilde{\gamma}^2}, \qquad (18)$$

where we have introduced a characteristic timescale $\tau_B = \beta/\pi$ associated with temperature $T = 1/k_B\beta$, see details of the derivation of the expression for the current in Appendix A. This perturbative expression for the current represents one of the central results of our paper.

As usual in the case of the Kubo formula, we have obtained an early time result. The expression of the current expectation value Eq. (17) allows us to calculate the current profile at short times. In the perturbative calculation, we assume that during time t the change in the QD occupation number is small. At high temperatures, the characteristic timescale is $t \ll \frac{1}{\tilde{\lambda}}(v\tau_B)^{\tilde{\gamma}^2/2}$, whereas at low temperatures it is given by $t \ll (\tilde{\lambda}^{-1} v^{\tilde{\gamma}^2/2})^{\frac{1}{1-\tilde{\gamma}^2/2}}$. The only dependence on the coupling $\tilde{\lambda}$ in the perturbative solution is an overall prefactor $\tilde{\lambda}^2$. Thus the shape of the perturbative current is independent of $\tilde{\lambda}$, which corresponds to the limit of small $\tilde{\lambda}$. Therefore, this approach cannot be used to calculate the change in an entire current pulse, since this requires integrating over all times. However, based on the arguments in Ref. [2], we know that this charge will be less than the electron or quasiparticle charge due to the interaction effects.

B. Noninteracting blip approximation for the spin-boson model

Using the Feynman-Vernon influence functional, the authors of Ref. [14] presented a path-integral solution for the time evolution of the reduced density matrix of the two-level system $\rho_{\sigma\sigma'}(t)$ by integrating out exactly the heat bath degrees of freedom. Using this density matrix, one can obtain the occupation of the dot $N(t)$ as well as the current profile $I(t)$. For a general initial condition $\rho_{\sigma_0\sigma_0'}(t_0)$, the time evolution of

the density matrix is given by the equation

$$\rho_{\sigma\sigma'}(t) = \int \mathcal{D}\sigma \mathcal{D}\sigma' \mathcal{A}[\sigma]\mathcal{A}^*[\sigma']\mathcal{F}[\sigma, \sigma']\rho_{\sigma_0\sigma_0'}(t_0), \quad (19)$$

where the integral is taken over all possible spin paths $\sigma(t)$. Here $\mathcal{A}[\sigma]$ is the probability amplitude for the system to follow the path $\sigma(t)$ in the absence of heat-bath fluctuations and $\mathcal{F}[\sigma, \sigma']$ is the Feynman-Vernon influence functional [14,49] which takes into account the heat bath, see Ref. [14]. Equation (19) is exact; however, to use it one has to evaluate the path integral over all possible spin paths. In practice, the path integral is turned into a sum over spin flips and we integrate over all possible times at which spin flips occur. In our numerical calculations, this series is truncated at a some fixed number of spin flips.

The initial condition for this procedure corresponding to the dot having initial occupation n_a is given by $\langle \sigma_z \rangle (t = 0) = 2n_a - 1$. Assuming the spin subsystem evolves from a pure state, it is shown in Ref. [14] that the time evolution reads

$$\langle \sigma_z(t) \rangle = (2n_a - 1)P_1^{(s)}(t) + P_1^{(a)}(t), \qquad (20)$$

where $P_1^{(s)}(t)$ and $P_1^{(a)}(t)$ are obtained from the series expansion in Δ. Each factor of Δ includes an additional time integral, hence limiting the maximum order of perturbation theory which we can evaluate numerically. Up to the second order in Δ, we have [50]

$$\begin{aligned}
P_1^{(s)}(t) = 1 - \int_0^t dt_2 \int_0^{t_2} dt_1 \Delta(t_2)\Delta(t_1) \cos(\Omega(t_1) - \Omega(t_2)) \\
\times e^{-Q'(t_2-t_1)} \cos(Q''(t_2 - t_1) + Q''(t_1) - Q''(t_2))
\end{aligned}$$

and

$$\begin{aligned}
P_1^{(a)}(t) = \int_0^t dt_2 \int_0^{t_2} dt_1 \Delta(t_2)\Delta(t_1) \sin(\Omega(t_1) - \Omega(t_2)) \\
\times e^{-Q'(t_2-t_1)} \sin(Q''(t_2 - t_1) + Q''(t_1) - Q''(t_2)).
\end{aligned}$$

The expansion to second order in Δ means that we consider paths with at most two spin flips. In the context of the spin-boson model, this truncation is called a NIBA. For an Ohmic heat bath with spectral function Eq. (11), the exact expressions for the functions $Q'(\tau)$ and $Q''(\tau)$ are given in Ref. [51], and which in the limit of small cutoff a read

$$Q'(\tau) = \alpha \ln(1 + (v\tau/a)^2) + 2\alpha \ln\left(\frac{\beta}{\pi\tau} \sinh(\pi\tau/\beta)\right), \qquad (21)$$

$$Q''(\tau) = 2\alpha \arctan(v\tau/a). \qquad (22)$$

These results together with Eq. (20) allow us to write an expression for the current in the form

$$\begin{aligned}
I(t) = \frac{\tilde{q}}{2}\Delta(t)\text{Re} \int_0^t d\tau \Delta(\tau)e^{-Q'(t-\tau)-iQ''(t-\tau)} \\
\times [2n_a \cos[\Omega(\tau) - \Omega(t)] - e^{i(\Omega(\tau)-\Omega(t))}]. \quad (23)
\end{aligned}$$

C. Showing equivalence of solutions

In this subsection, we will show that the current profile that was calculated using perturbation theory Eq. (17) is equivalent to the result of the NIBA of the spin-boson model Eq. (23).
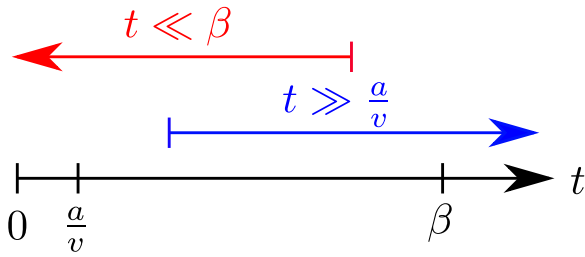
FIG. 2. Sketch showing that the whole of t-space can be divided into two regimes which overlap: the $t \gg \frac{a}{v}$ regime and the $t \ll \beta$ regime due to the fact that $\frac{a}{v} \lll \beta$. Since we prove the identity Eq. (24) in both limits, we have proven it for all t.

First, we want to show that Q' and Q'' from Sec. III B are related to the propagator Φ from Sec. III A by

$$\Phi(t) = \frac{1}{2\pi} a^{-\tilde{\gamma}^2} e^{-Q'(t) - iQ''(t)}. \tag{24}$$

Since $\Phi^*(t) = \Phi(-t)$ and $Q'(t) = Q'(-t)$ and $Q''(t) = Q''(-t)$, we can focus on the case $t > 0$. The important thing to realize is that $\frac{a}{v} \lll \beta$, since a is a small distance cutoff and the experimentally relevant regime is at low temperatures. Therefore the whole of t-space can be divided into two regimes which overlap: the $t \gg \frac{a}{v}$ regime and the $t \ll \beta$ regime, see Fig. 2. From Eq. (18) and from Eqs. (21) and (22) it is easy to show that Eq. (24) is satisfied in both limits. Hence we have proven their equality for all t. The identity Eq. (24) can also be viewed as a consequence of the bosonization formalism, it is equivalent to Eq. (78) in Ref. [44].

One can then show that Eqs. (17) and (23) are identical. We prove this in Appendix C. We also prove that the current can be written in the more useful form

$$I(t) = \frac{\tilde{q}}{2} \Delta(t) \int_0^t d\tau \, \Delta(t - \tau)$$
$$\times \frac{\cos\left(2\alpha \arctan \frac{v\tau}{a} + \Omega(t-\tau) - \Omega(t)\right)}{(1 + (v\tau/a)^2)^\alpha \left(\frac{\beta}{\pi\tau} \sinh \frac{\pi\tau}{\beta}\right)^{2\alpha}}. \tag{25}$$

Since both solutions are entirely equivalent, when we refer to the perturbative solution in the text below, we are referring to either of the two solutions Eqs. (17) or (23).

IV. NONPERTURBATIVE APPROACHES

The two equivalent solutions we outlined above were both perturbative in the spin-bath coupling; however, they were applicable for all α. There are two special values of α for which we can go further and solve the problem to all orders in the coupling Δ. In this section, we briefly outline these two approaches and then show numerical data comparing the perturbative solution Eq. (23) to these exact methods. We show that at early times the perturbative solution gives very accurate results and can therefore be used to model the experimental setup of Ref. [37].

The value $\alpha = 1/2$ is special, because it corresponds to the case in which we have an integer quantum Hall edge [52]. This means that we have a free fermion on the boundary and we can solve the problem exactly. This solution has been derived by

previous authors [53,54], however, we present an alternative derivation in Appendix D.

There is a further special point $\alpha = 0$, in which case the QD decouples completely from the edge and the problem becomes trivial. If we are close to this point, viz. $\alpha \ll 1$, then the entire perturbative expansion in Δ can be resummed as shown in Ref. [15]. The evolution of the dot is then given by the GME. For more details of this approach, also see Ref. [2].

We expect the perturbative solution to be valid at short times, for $t\Delta < 1$. In Fig. 3, we present our numerical results for the current and the occupation number on the QD after a linear voltage ramp with the rate ξ, so $\varepsilon(t) = \xi(t - t_0)$. In this protocol, the dot is occupied in the initial state. At early times, $\varepsilon(t)$ is negative and so only very little charge leaks off the dot as the dot equilibrates with the edge. For times $t > t_0$ the bias becomes positive and the current greatly increases. The current shows oscillatory behavior with increasing frequency as the bias increases with time. These are the characteristic Rabi oscillations.

Figure 3(b) shows the case $\alpha = 1/2$, corresponding to a $\nu = 1$ integer QHE state. We compare the exact solution (D17) to the perturbative result and find a good agreement at early times. At later times, the perturbative result misses the exponential decay of the current on the timescale $1/\Delta$. The inset shows that the occupation is initially very close to unity when $\varepsilon(t) < 0$ and then starts decreasing once $\varepsilon(t) > 0$.

Figure 3(c) shows the result for $\alpha = 0.01$, in which case the GME is expected to be a good approximation at all times. Our perturbative result agrees with the GME at early times as expected. For $t\Delta > 5$, we start seeing a discrepancy between the two curves since the occupancy of the dot is starting to differ significantly from 1 and the corresponding feedback effect leads to higher-order corrections to the current that our perturbation theory misses. Again, the inset shows the dot to be fully occupied until $\varepsilon(t)$ becomes positive. At late times, the dot occupation tends to the Landau-Zener result [2]. Comparing the $\alpha = 0.01$ results to the $\alpha = 1/2$ results, we see that the amplitude of the Rabi oscillations is strongly suppressed in the latter case. This is consistent with the crossover of the spin-boson model at $\alpha = 1/2$ from the coherent to the incoherent regime. In the coherent regime there are strong oscillations, whereas in the incoherent regime the spin changes monotonically after a quench [7,8].

Hence we see that in the two limits of α where we have access to simple solutions that are valid for all times, our perturbative result gives a good approximation to the current at early times. However, for other values of α which may be experimentally relevant, no such simple solution schemes exist and here the perturbative solution Eq. (17) or, equivalently, the NIBA, is useful.

V. ANALYTICAL LIMITS OF THE CURRENT PROFILE

In this section, we show that we can obtain analytical expressions for the perturbative current profile Eq. (23) in a number of parameter regimes. We have three timescales [55] in our perturbation theory result:

$$\tau_B = \frac{\beta}{\pi}, \quad \frac{1}{\Omega} = (\partial \ln \varepsilon / \partial t)^{-1}, \quad \frac{1}{\varepsilon_0}. \tag{26}$$
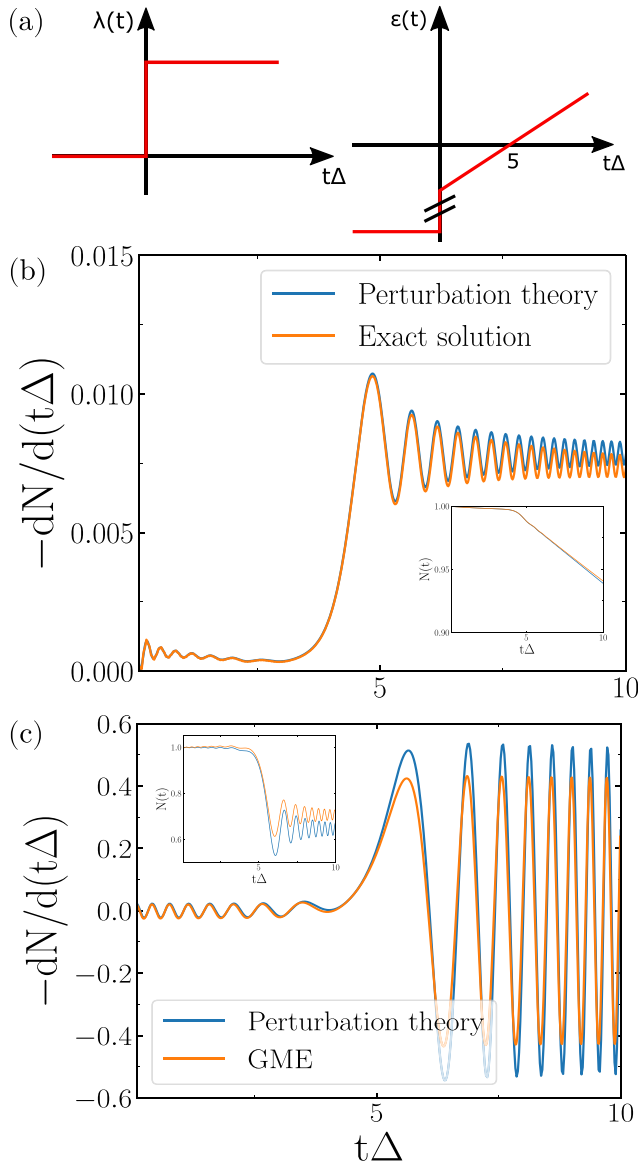
FIG. 4. Comparison of the full solution Eq. (25) with the analytical expression Eq. (29), which is valid in the limit $\varepsilon_0 \ll \Omega$. We show the time evolution of the current when the dot is driven with a bias $\varepsilon(t) = \varepsilon_0 \cos \Omega t$. We use the parameters $\Omega = 5\Delta$, $a = 0.01 v\Delta^{-1}$, and $\varepsilon_0 = 0.1\Delta$. The agreement between the solutions is excellent as long as $vt \gg a$.

(but remains weak). The particle leaks slowly off onto the edge.

We consider general $\alpha = \frac{1}{2\nu}$ as appropriate for the case where an electron (as opposed to a quasielectron) is tunneling. In the zero bias case $\varepsilon(t) = 0$, although we only have the early time current using perturbation theory, we can extend the integration limit in Eq. (23) to infinity, since the integrand vanishes quickly as $\tau \gg \frac{a}{v}$ [57]. This integral is solved in [5]

$$I_0 = \frac{\tilde{q}}{\pi v}(2n_a - 1)\tilde{\lambda}^2 \frac{\sqrt{\pi}}{2} \frac{\Gamma(\alpha)}{\Gamma(\alpha + \frac{1}{2})} \left(\frac{\pi k_B T}{v}\right)^{2\alpha - 1}, \quad (27)$$

$$\frac{I_0}{\tilde{q}} \begin{cases} > 0 & n_a > 1/2 \\ = 0 & n_a = 1/2 \\ < 0 & n_a < 1/2. \end{cases} \quad (28)$$

This makes sense from a physical point of view, the occupation number of the dot tends to $n_a = \frac{1}{2}$ as it reaches thermal equilibrium with the edge.

We note that in Eq. (27) the zero temperature limit is well defined for $\alpha \geqslant 1/2$. On the other hand, for $\alpha < 1/2$ we require a finite temperature as an infrared cutoff.

B. Zero temperature, sinusoidal bias, $\alpha = \frac{3}{2}$

Experiments must be performed at temperatures well below the FQH gap and therefore the zero temperature limit is the most relevant. Focusing on the $\nu = 1/3$ particle case, when $\beta \to \infty$ the expression Eq. (25) simplifies. Let $\varepsilon(t) = \varepsilon_0 \cos \Omega t$ and assume that $vt \gg a$ and $\varepsilon_0 \ll \Omega$ so we can obtain the approximate form

$$I(t) = \frac{\tilde{q}\tilde{\lambda}^2}{2v^3} \frac{\Omega}{\pi} \varepsilon_0 \left(\left[\ln\left(\frac{a\Omega}{v}\right) + \gamma_E \right] \sin \Omega t + \frac{\pi}{2} e^{a\Omega/v} \cos \Omega t \right), \quad (29)$$

where $\gamma_E \approx 0.577$ is the Euler-Mascheroni constant. We derive this result in detail in Appendix E. We compare this analytical expression with the full integral expression Eq. (25) in the numerics presented in Fig. 4 and see excellent agreement.

FIG. 3. Comparison of the perturbative solution Eq. (17) with two nonperturbative methods. We show the time evolution of the current after a linear ramp $\varepsilon(t) = \xi(t - t_0)$ with parameters $a = 0.005 v\Delta^{-1}$, $\xi = 4\Delta^2$, $t_0 = 5\Delta^{-1}$. We plot $-dN/d(t\Delta)$, where $N(t) = \langle \hat{N}(t) \rangle$. The insets show the time evolution of the occupation number $N(t)$ on the QD. (a) Sketch of the sweep protocol. (b) For $\alpha = 1/2$, we compare the exact solution as derived in Appendix D (yellow) with our perturbative result (blue). (c) For $\alpha = 0.01$, we compare the result from the GME (yellow) with our perturbative result (blue). Detailed expressions for the GME are given in Ref. [2]. In both cases, the early time agreement between the solutions is excellent.

$\frac{1}{\Omega}$ is the typical timescale on which the bias $\varepsilon(t)$ varies and ε_0 is the maximum amplitude of the bias. We assume the all the associated energy scales are much smaller than the FQH gap, which is of order 1meV for $\nu = 1/3$ [56].

A. Zero bias result

In this setup, a particle starts on the dot at zero bias $\varepsilon = 0$ and the tunneling is turned on suddenly at $t = 0$
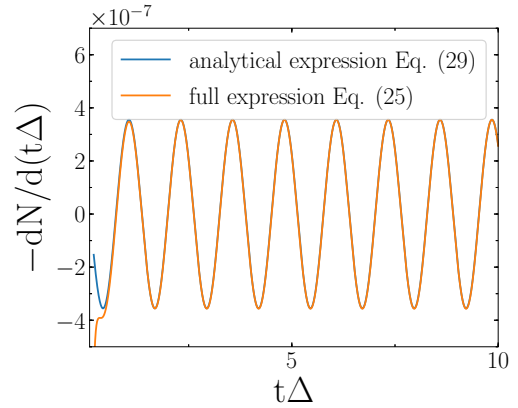
From this result, we see that we will obtain a periodic current with a phase shift relative to the driving bias. We expect this phase shift to be an experimentally accessible signature.

We note that there is a logarithmic dependence on the cutoff a in the expression Eq. (29). This cutoff dependence is a generic feature for $\alpha > 1/2$. Indeed, a similar behavior is seen in numerical simulations of the spin-boson model using tensor network methods [58]. We can show explicitly that the results do not depend on the cutoff when $\alpha \leqslant 1/2$.

VI. CONCLUSION

In this paper, we derived in detail the relations between the QD problem and the spin-boson model. The bosonized edge in the QD problem maps to the bosonic heat bath of the spin-boson model. The QD corresponds to the two-state system of the spin-boson model. We have perturbatively calculated the current arising when a QD is coupled to an FQH edge. We performed the calculations using the two alternative descriptions. To lowest order in perturbation theory in the spin-bath coupling λ, the solution obtained by bosonization of the original Hamiltonian is shown to be equivalent to the solution by mapping to the spin-boson model. This provides a consistency check of the map.

Our approach provides a very simple expression that can be used to compare to experimental results. We have shown that the perturbative calculation on the bosonized Hamiltonian agrees very well with two nonperturbative techniques. First, the GME is a method for solving the spin-boson model when the coupling α is small. Second, we derive an exact solution of the noninteracting (IQH) problem. Numerical simulations show that as long as the occupation number on the dot stays close to its initial value, the agreement with our perturbative method is excellent. However, these exact methods are only valid in a limited parameter regime of the coupling α. The perturbative solution is valid over the full parameter range of the spin-boson model, i.e., any α.

For a periodic bias $\varepsilon(t)$ applied to the QD, there is a phase shift between the bias $\varepsilon(t)$ and the resulting current $I(t)$. This theoretical prediction is verifiable experimentally. To perform the experiment, either the current on the edge after the dot can be measured directly or other indirect methods can be used. For example, one can couple a second quantum dot to the edge and drive it out of phase with the first dot to obtain zero current after the dot. An analogous experiment where the particle emitted by the quantum dot is reabsorbed by a quantum dot further along the channel was described for the IQH case in Ref. [59].

Our perturbative calculation has also confirmed (see Appendix B) that neglecting the Klein factors in the bosonization prescription yields the correct answer for this model.

We compared our prediction that the integrated charge in a current pulse is renormalized away from $-e$ due to Coulomb interactions to the experiment in Ref. [37]. In particular, Fig. 1 B of Ref. [37] shows the time-dependent current on the edge. That experiment is performed for an integer quantum Hall edge, i.e., $\nu = 1$, hence, naively we would expect $\alpha = 1/2$. However, as emphasized in Ref. [2] and again in this paper, the Coulomb interactions between the dot and the edge will renormalize α to a different value. We searched for evidence of this interaction effect in the experimental data of Ref. [37]; however, unfortunately the error bars on the experiment are too large to detect the presumably small deviation from $\alpha = 1/2$. We believe, however, that the effect is large enough that it would be seen in experiments with improved accuracy.

Further theoretical work could be devoted to using the powerful numerical techniques—such as the stochastic Schrödinger equation—developed for the spin-boson model to model the QD in experimentally relevant regimes. Recently, there has been a proposal to use tensor networks to study the spin-boson model [18].

Another possibility for further theoretical research would be to make use of the mapping to the Kondo problem to explore the Kondo regime of this problem more carefully. This problem should be tractable with DMRG techniques.

In compliance with EPSRC policy framework on research data, this publication is theoretical work that does not require supporting research data.

APPENDIX A: DETAILED PERTURBATION THEORY CALCULATIONS

In this Appendix, we will derive the current profile Eq. (17) using perturbation theory in detail. With the help of the spin commutation relations, we can derive explicitly the current operator from the Heisenberg Eq. (14):

$$\hat{I}(t) = -i\tilde{q}\tilde{\lambda}(t)(\hat{\tilde{\psi}}^\dagger(0,t)\hat{S}^-(t) - \hat{S}^+(t)\hat{\tilde{\psi}}(0,t)). \quad (A1)$$

Combining Eq. (A1) with the Kubo formula Eq. (16), we obtain the current expectation value at time t as

$$I(t) = -\tilde{q}\tilde{\lambda}(t)\int_0^t \tilde{\lambda}(t')\langle[\hat{S}^-(t)\hat{\tilde{\psi}}^\dagger(0,t), \hat{S}^+(t')\hat{\tilde{\psi}}(0,t')]$$
$$- [\hat{S}^+(t)\hat{\tilde{\psi}}(0,t), \hat{S}^-(t')\hat{\tilde{\psi}}^\dagger(0,t')]\rangle\,dt'. \quad (A2)$$

In the interacting picture, the operators evolve with time under $H_0(t)$,

$$\hat{S}^-(t) = e^{-i\Omega(t)}\hat{S}^-(0), \quad \hat{S}^+(t) = e^{i\Omega(t)}\hat{S}^+(0), \quad (A3)$$

where $\Omega(t) = \int_0^t \varepsilon(s)\,ds$. Combining Eqs. (A2) and (A3) and defining the fermionic propagators

$$\Phi_{+-}(\tau) = \langle\hat{\tilde{\psi}}(0,\tau)\hat{\tilde{\psi}}^\dagger(0,0)\rangle, \quad (A4)$$

$$\Phi_{-+}(\tau) = \langle\hat{\tilde{\psi}}^\dagger(0,\tau)\hat{\tilde{\psi}}(0,0)\rangle, \quad (A5)$$

we obtain the result

$$I(t) = -\tilde{q}\tilde{\lambda}(t)\int_0^t dt'\tilde{\lambda}(t')(e^{i\Omega(t')-i\Omega(t)}[(1-n_a)\Phi_{-+}(t-t') - n_a\Phi_{+-}(t'-t)]$$
$$+ e^{-i\Omega(t')+i\Omega(t)}[-n_a\Phi_{+-}(t-t') + (1-n_a)\Phi_{-+}(t'-t)]) \tag{A6}$$

using the time-translational invariance of the propagator. Using the explicit form of fermion operator $\hat{\tilde{\psi}}$ in bosonization language Eq. (5) and the result for two point functions of vertex operators in Ref. [44],

$$\langle e^{i\tilde{\gamma}\hat{\phi}(\tau)}e^{-i\tilde{\gamma}\hat{\phi}(0)}\rangle = \left(\frac{a}{v\tau_B\sin\left(\frac{iv\tau+a}{v\tau_B}\right)}\right)^{\tilde{\gamma}^2}, \tag{A7}$$

we can show that

$$\Phi_{+-}(\tau) = \frac{1}{2\pi}\left(\frac{1}{iv\tau_B\sinh\left(\frac{v\tau-ia}{v\tau_B}\right)}\right)^{\tilde{\gamma}^2}. \tag{A8}$$

One can also show that $\Phi_{+-}(\tau) = \Phi_{-+}(\tau) \equiv \Phi(\tau)$ [60], which converts Eq. (A6) to the final result Eq. (17).

APPENDIX B: KLEIN FACTORS AND (ANTI)COMMUTATION RELATIONS

In the above calculation, we have neglected the Klein factors. The reason is that we only have one chiral edge and

we are calculating the current. Klein factors become important when we have different species of particles. In perturbation theory, at all orders we have an equal number of $\hat{\psi}$ and $\hat{\psi}^\dagger$ in the expectation values and the Klein factors cancel,

$$\hat{\tilde{\psi}}(x) = \frac{1}{\sqrt{2\pi}}a^{-\frac{\tilde{\gamma}^2}{2}}\hat{F}e^{-i\tilde{\gamma}\hat{\phi}(x)}, \tag{B1}$$

where the Klein factors $\hat{F}$ satisfy [44]

$$[\hat{F}, \hat{b}_k] = 0, \quad [\hat{F}, \hat{\mathcal{N}}] = \hat{F} \text{ and } \hat{F}^\dagger\hat{F} = 1, \tag{B2}$$

where $\hat{\mathcal{N}}$ is the total number operator on the edge. Now if we substitute the expression Eq. (B1) into Eq. (A2), then we can commute the Klein factors past the spin operators and use $\hat{F}^\dagger\hat{F} = 1$ to eliminate the Klein factors.

We also note that if we replace the spin operators by ladder operators, viz. $\hat{S}^+ = \hat{a}^\dagger$, then the Klein factors need to be commuted past both $\hat{a}$ and $\hat{a}^\dagger$ in Eq. (A2) and so any statistical phase will cancel out.

APPENDIX C: EQUIVALENCE OF TWO SOLUTIONS: DETAILS OF THE DERIVATION

We start off with the expression Eq. (17):

$$I(t) = -\tilde{q}\int_0^t dt'\tilde{\lambda}(t)\tilde{\lambda}(t')(e^{i\Omega(t')-i\Omega(t)}[(1-n_a)\Phi(t-t') - n_a\Phi(t'-t)] + e^{i\Omega(t)-i\Omega(t')}[(1-n_a)\Phi(t'-t) - n_a\Phi(t-t')]). \tag{C1}$$

Substitute in the expression for Φ and use the fact that $Q'(t) = Q'(-t)$ and $Q''(t) = -Q''(-t)$ to find

$$I(t) = -\frac{\tilde{q}}{2\pi}a^{-\tilde{\gamma}^2}\int_0^t dt'\tilde{\lambda}(t)\tilde{\lambda}(t')e^{-Q'(t-t')}(e^{i\Omega(t')-i\Omega(t)}[(1-n_a)e^{-iQ''(t-t')} - n_ae^{iQ''(t-t')}] + \text{c.c.}), \tag{C2}$$

where c.c. denotes the complex conjugate. We can sum the exponential to get and use $\Delta^2 = \tilde{\lambda}^2\frac{2}{\pi}a^{-\tilde{\gamma}^2}$ to get

$$I(t) = -\frac{\tilde{q}}{2}\int_0^t dt'\Delta(t)\Delta(t')e^{-Q'(t-t')}([(1-n_a)\cos(\Omega(t')-\Omega(t)-Q''(t-t')) - n_a\cos(\Omega(t')-\Omega(t)+Q''(t-t'))). \tag{C3}$$

Going back to exponential notation:

$$I(t) = -\frac{\tilde{q}}{2}\mathfrak{Re}\int_0^t dt'\Delta(t)\Delta(t')e^{-Q'(t-t')-iQ''(t-t')}([1-n_a]e^{i\Omega(t')-i\Omega(t)} - n_ae^{-i\Omega(t')+i\Omega(t)}), \tag{C4}$$

$$I(t) = \frac{\tilde{q}}{2}\mathfrak{Re}\int_0^t dt'\Delta(t)\Delta(t')e^{-Q'(t-t')-iQ''(t-t')}(2n_a\cos(\Omega(t')-\Omega(t)) - e^{-i\Omega(t')+i\Omega(t)}). \tag{C5}$$

Finally, renaming t' to τ, we obtain the desired expression Eq. (23). We also want to derive another useful expression. For $n_a = 1$, we obtain from Eq. (C3):

$$I(t) = \frac{\tilde{q}}{2}\int_0^t dt'\Delta(t)\Delta(t')e^{-Q'(t-t')}\cos(\Omega(t')-\Omega(t)+Q''(t-t')). \tag{C6}$$

Defining $\tau = t - t'$ and substituting in the expressions Eqs. (21) and (22) for Q' and Q'', respectively, we find

$$I(t) = \frac{\tilde{q}}{2}\Delta(t)\int_0^t d\tau\Delta(t-\tau)\frac{\cos\left(2\alpha\arctan\frac{v\tau}{a} + \Omega(t-\tau) - \Omega(t)\right)}{(1+(v\tau/a)^2)^\alpha\left(\frac{\beta}{\pi\tau}\sinh\frac{\pi\tau}{\beta}\right)^{2\alpha}}, \tag{C7}$$

and the zero bias result is

$$I_0(t) = \frac{\tilde{q}}{2}\Delta(t)\int_0^t d\tau \, \Delta(t-\tau)\frac{\cos\left(2\alpha \arctan \frac{v\tau}{a}\right)}{(1+(v\tau/a)^2)^\alpha \left(\frac{\beta}{\pi\tau}\sinh\frac{\pi\tau}{\beta}\right)^{2\alpha}}. \tag{C8}$$

For $\alpha = (2n+1)/2$ and $\Delta(t) = \theta(t)$, this $I_0(t)$ tends to a constant on the short timescale a/v:

$$I_0 = \frac{\tilde{q}}{2}\Delta^2 \int_0^\infty d\tau \frac{\cos\left(2\alpha \arctan \frac{v\tau}{a}\right)}{(1+(v\tau/a)^2)^\alpha \left(\frac{\beta}{\pi\tau}\sinh\frac{\pi\tau}{\beta}\right)^{2\alpha}}. \tag{C9}$$

Adding and subtracting I_0 from Eq. (C7), we obtain

$$I(t) = I_0 + \frac{\tilde{q}}{2}\Delta(t)\int_0^t d\tau \, \Delta(t-\tau)\frac{1}{(1+(v\tau/a)^2)^\alpha}\frac{\cos\left(2\alpha \arctan \frac{v\tau}{a}+\Omega(t-\tau)-\Omega(t)\right)-\cos\left(2\alpha \arctan \frac{v\tau}{a}\right)}{\left(\frac{\beta}{\pi\tau}\sinh\frac{\pi\tau}{\beta}\right)^{2\alpha}}. \tag{C10}$$

APPENDIX D: EXACT SOLUTION FOR IQH

This section presents an exact solution valid at the special point $\alpha = 1/2$. The same result has been derived by previous authors using different methods, either by considering small time slices over which the bias is constant [53] or by calculating the S matrix [54]. Here, we present an alternative method of calculating this result.

In this section, we represent the dot by fermionic creation and annihilation operators $\hat{a}^\dagger$ and $\hat{a}$. The transformation from fermions to spin $1/2$ allows us to map between this representation and the spin representation used in the main text. In the integer case and in the absence of Coulomb interactions, the Hamiltonian is

$$\hat{H} = \hat{H}_0 + \hat{H}_{\text{tun}}, \tag{D1}$$

where

$$\hat{H}_0 = -iv\int_{-L/2}^{L/2}\hat{\psi}^\dagger(x)\partial_x\hat{\psi}(x)\,dx + \varepsilon(t)\hat{a}^\dagger(t)\hat{a}(t) \tag{D2}$$

is the free Hamiltonian. The first term of Eq. (D2) describes the dynamics of an IQH edge with length L at filling fraction $\nu = 1$ [61]. Wen showed in Ref. [43] that the edge modes of the IQH fluid are described by a free chiral fermion $\hat{\psi}$ whose velocity v depends on the confining potential. The second term of Eq. (D2) represents the QD which we model as a time-dependent energy level $\varepsilon(t)$. The coupling between the IQH edge and the QD is modeled by the interaction term

$$\hat{H}_{\text{tun}}(t) = \lambda(t)\hat{\psi}^\dagger(0)\hat{a} + \text{H.c.} \tag{D3}$$

To emphasize the position of the contact at $x = 0$, we decompose the fermion field $\psi(x,t)$ into the left and right components,

$$\hat{\psi}(x,t) = \hat{\psi}_L(x,t)\Theta(-x) + \hat{\psi}_R(x,t)\Theta(x), \tag{D4}$$

where $\Theta(x)$ is the Heaviside step function and we use the convention $\Theta(0) = 1/2$ to symmetrize the contribution of the left and right parts at the contact point. From the Hamiltonian Eq. (D1), we derive the field equations

$$i\partial_t\hat{a}(t) = \frac{\lambda(t)}{2}(\hat{\psi}_L(0,t) + \hat{\psi}_R(0,t)) + \varepsilon(t)\hat{a}(t), \tag{D5}$$

$$i\dot{\hat{\psi}}(y,t) = -iv\partial_y\hat{\psi}(y,t) + \lambda(t)\delta(y)\hat{a}(t), \tag{D6}$$

where we have already used the decomposition Eq. (D4). Integrating Eq. (D6) from $-\epsilon$ to $+\epsilon$, we arrive at the constraint [62]:

$$0 = iv(\hat{\psi}_R(0,t) - \hat{\psi}_L(0,t)) - \lambda(t)\hat{a}(t). \tag{D7}$$

With the help of Eq. (D7), we can eliminate $\hat{\psi}_R$ from Eq. (D5) and arrive at

$$i\partial_t\hat{a}(t) = \frac{\lambda(t)}{2}\left(2\hat{\psi}_L(0,t) - i\frac{\lambda(t)}{v}\hat{a}(t)\right) + \varepsilon(t)\hat{a}(t). \tag{D8}$$

Since the IQH edge is described by a chiral fermion $\hat{\psi}$, the appearance of the QD only affects the right component of the IQH edge [63]. With this observation, we can expand $\hat{\psi}_L(x,t)$ in terms of free modes

$$\hat{\psi}_L(x,t) = \frac{\sqrt{L}}{v}\int_{-\infty}^\infty \frac{d\omega}{2\pi}e^{i\omega(\frac{x}{v}-t)}\hat{c}_\omega, \tag{D9}$$

where the fermion operator $\hat{c}_\omega$ annihilates a chiral mode at energy ω on the IQH edge. Substituting Eq. (D9) into Eq. (D8) and using the ansatz

$$\hat{a}(t) = g(t)\hat{a}(0) + \int_{-\infty}^\infty \frac{d\omega}{2\pi}f_\omega(t)\hat{c}_\omega, \tag{D10}$$

we obtain differential equations for $g(t)$ and $f_\omega(t)$. Solving these differential equations, we derive the exact solution

$$g(t) = e^{-\xi(t)}, \tag{D11}$$

$$f_\omega(t) = -i\frac{\sqrt{L}}{v}\int^t dt'\lambda(t')e^{-i\omega t'+\xi(t')-\xi(t)}, \tag{D12}$$

where we have defined

$$\xi(t) = \int_{-\infty}^t \left[i\varepsilon(s) + \frac{\lambda(s)^2}{2v}\right]ds. \tag{D13}$$

In the next section, we set $\lambda(t) = \lambda\Theta(t)$ for conciseness. In that case, we define $\Omega(t) = \int_0^t \varepsilon(t)\,dt$ and the timescale

$$\tau_0 = \frac{v}{\lambda^2}, \tag{D14}$$

which is the timescale over which a current from the dot to the edge decays and it can hence be viewed as a tunneling timescale. With this result, we are able to derive the quantities that can be measured in the physical setup with the general applied bias voltage $\varepsilon(t)$.

We define the current operator via Eq. (14). From the exact time-dependent operator $\hat{a}$ Eq. (D10), we can derive the expectation value of the current at any given time $I(t) = \langle \hat{I}(t) \rangle$ using the Heisenberg picture. To calculate the expectation value of the time-dependent operator, we need to set the initial condition of the QD and introduce the Fermi distribution on the IQH edge,

$$\langle \hat{a}^\dagger(0)\hat{a}(0) \rangle = n_a, \tag{D15}$$

$$\langle \hat{c}_{\omega'}^\dagger \hat{c}_\omega \rangle = \frac{2\pi v}{L}\delta(\omega - \omega')n_F(\omega), \tag{D16}$$

where $n_F(\omega) = (e^{\beta\omega} + 1)^{-1}$ is the Fermi distribution and we define $\beta = 1/k_B T$ as usual. To obtain sensible results, we need to introduce a cutoff frequency $\omega_c \gg k_B T$, which adds a factor e^{ω/ω_c} to the frequency integrals. This cutoff makes sense physically since the negative frequency fermion modes, which are deep inside the Fermi sea, do not affect the low-energy physics near the chemical potential. We write this in the suggestive form $\omega_c = v/a$. Combining the exact solution Eq. (D10) and the definition Eq. (14), after some algebraic calculations, we obtain

$$I(t) = q\frac{\lambda(t)^2}{v}\mathfrak{Re}\left\{ e^{-2\mathfrak{Re}\xi(t)}n_a - \frac{e^{-2\mathfrak{Re}\xi(t)}}{v}\int_{-\infty}^t dt' \int_{-\infty}^t dt'' \lambda(t')\lambda(t'')\frac{1}{2\pi}\frac{\pi i}{\beta}\frac{e^{\xi(t')+\xi^*(t'')}}{\sinh\left(\frac{\pi}{\beta}\left(t''-t'-\frac{ia}{v}\right)\right)} \right.$$
$$\left. + 2\int_{-\infty}^t dt'\frac{1}{2\pi}\frac{\pi i}{\beta}\frac{e^{\xi(t')-\xi(t)}}{\sinh\left(\frac{\pi}{\beta}\left(t-t'-\frac{ia}{v}\right)\right)} \right\}. \tag{D17}$$

We can show explicitly that our space cutting solution obeys charge conservation. We have the operator identity [64]

$$i\partial_t(\hat{a}^\dagger a) = i\hat{a}^\dagger \partial_t \hat{a} + i(\partial_t \hat{a}^\dagger)\hat{a}. \tag{D18}$$

Combining the above equation with Eq. (D5) and its complex conjugate, we obtain

$$i\partial_t(\hat{a}^\dagger a) = \frac{\lambda}{2}(\hat{a}^\dagger(\hat{\psi}_R + \hat{\psi}_L) - (\hat{\psi}_R^\dagger + \hat{\psi}_L^\dagger)a). \tag{D19}$$

Now replacing $\hat{a}$ and $\hat{a}^\dagger$ using Eq. (D7), we find

$$\partial_t(\hat{a}^\dagger a) = v(\hat{\psi}_L^\dagger \hat{\psi}_L - \hat{\psi}_R^\dagger \hat{\psi}_R), \tag{D20}$$

which is nothing but the charge conservation equation. The left-hand side of Eq. (D20) is the time variation of total charge on the QD. The right-hand side of Eq. (D20) is the total current from the IQH edge to the dot since the current that goes into the contact point is $v(\hat{\psi}_L^\dagger \hat{\psi}_L)$ and the current that goes out of it is $v(\hat{\psi}_R^\dagger \hat{\psi}_R)$. If we add the Coulomb interaction term $H_{int} \propto \hat{\psi}^\dagger(0)\hat{\psi}(0)\hat{a}^\dagger a$ to the Hamiltonian, then the equation of motion Eq. (D6) is modified. However, it is easy to show that even then, the charge conservation Eq. (D20) is still satisfied.

We now compare the exact solution to our perturbative result Eq. (17). Setting $\tilde{\gamma} = 1$ in Eq. (18) and using the assumption $v\tau_B/a \to \infty$, we obtain $\mathfrak{Re}\Phi(t-t') = \frac{1}{2v}\delta(t-t')$. Setting $\lambda(t) = \lambda\Theta(t)$, we find the final result for the case $\tilde{\gamma} = 1$,

$$I(t) = \frac{qn_a\lambda^2}{v} + \frac{q\lambda^2}{\pi v}\mathfrak{Re}\left[\int_0^t dt' e^{i\Omega(t')-i\Omega(t)} \right.$$
$$\left. \times \frac{\pi i}{\beta}\frac{1}{\sinh\left(\frac{\pi(t-t')}{\beta} - i\frac{\pi a}{\beta v}\right)} \right], \tag{D21}$$

where we have used $\Theta(0) = 1/2$. If we expand the exact solution Eq. (D17) to second order in λ, then Eq. (D21) is obtained, so indeed both methods agree. This equivalence is a nontrivial cross-check of our perturbation theory method.

APPENDIX E: DERIVATION OF THE ANALYTICAL EXPRESSION FOR THE CURRENT

For conciseness, we define the frequency scale $\omega_c = v/a$. When $\beta \to \infty$, the expression Eq. (25) simplifies to

$$I(t) = \frac{e\Delta^2}{4}\int_0^t d\tau \frac{\cos(3\arctan(\omega_c\tau) + \Omega(t-\tau) - \Omega(t))}{(1+(\omega_c\tau)^2)^{3/2}}. \tag{E1}$$

Define

$$\zeta(t-\tau, t) = \Omega(t-\tau) - \Omega(t). \tag{E2}$$

Now assume that $\epsilon_0 \ll \Omega$ so $\zeta \ll 1$ and we can expand the trigonometric functions:

$$I(t) = \frac{e\Delta^2}{4}\int_0^t \frac{d\tau}{(1+(\omega_c\tau)^2)^{3/2}}$$
$$\times (\cos(3\arctan(\omega_c\tau))\cos\zeta(t-\tau, t)$$
$$- \sin(3\arctan(\omega_c\tau))\sin\zeta(t-\tau, t)), \tag{E3}$$

$$I(t) \approx \frac{e\Delta^2}{4}\int_0^t \frac{d\tau}{(1+(\omega_c\tau)^2)^{3/2}}(\cos(3\arctan(\omega_c\tau))$$
$$- \sin(3\arctan(\omega_c\tau))\zeta(t-\tau, t)). \tag{E4}$$

Now use the trigonometric identities

$$\cos(3\arctan x) = \frac{1-3x^2}{(1+x^2)^{3/2}}, \tag{E5}$$

$$\sin(3\arctan x) = \frac{3x - x^3}{(1+x^2)^{3/2}}, \tag{E6}$$

so with $\epsilon(t) = \epsilon_0\cos\Omega t$,

$$I(t) \approx \frac{e\Delta^2}{4}\int_0^t \frac{d\tau}{(1+(\omega_c\tau)^2)^3}\left[1 - 3(\omega_c\tau)^2 \right.$$
$$- \frac{\epsilon_0}{\Omega}(3\omega_c\tau - (\omega_c\tau)^3)(\sin\Omega t(1 - \cos\Omega\tau)$$
$$\left. + \cos\Omega t\sin\Omega\tau) \right], \tag{E7}$$

and rescaling the integration variable

$$I(t) \approx \frac{e\Delta^2}{4\omega_c} \int_0^{\omega_c t} \frac{dx}{(1+x^2)^3} \left[1 - 3x^2 - \frac{\epsilon_0}{\Omega}(3x - x^3) \right.$$
$$\left. \times \left(\sin \Omega t \left(1 - \cos \frac{\Omega}{\omega_c} x \right) + \cos \Omega t \sin \frac{\Omega}{\omega_c} x \right) \right] \quad \text{(E8)}$$

and

$$I(t) = I_0(t) + I_1(t) \sin \Omega t + I_2(t) \cos \Omega t, \quad \text{(E9)}$$

where

$$I_0(t) = \frac{e\Delta^2}{4\omega_c} \int_0^{\omega_c t} dx \frac{1 - 3x^2}{(1+x^2)^3} = \frac{e\Delta^2}{4\omega_c} \frac{\omega_c t}{(1 + (\omega_c t)^2)^2}$$
$$\approx \frac{\Delta^2}{4\omega_c} \frac{1}{(\omega_c t)^3} \to 0 \quad \text{(E10)}$$

as $\omega_c t \to \infty$. Now

$$I_1(t) = \frac{e\Delta^2}{4\omega_c} \frac{\epsilon_0}{\Omega} \int_0^{\omega_c t} dx \frac{(3x - x^3)\left(1 - \cos \frac{\Omega}{\omega_c}x\right)}{(1+x^2)^3}. \quad \text{(E11)}$$

Since $\omega_c t \gg 1$ and the integrand dies off at large x, we can extend the upper limit of the integral to ∞. Then this integral can be done exactly in terms of the Meijer G-function. We can expand this for $\frac{\Omega}{\omega_c} \ll 1$:

$$I_1(t) = \frac{e\Delta^2}{4\omega_c} \frac{\epsilon_0}{\Omega} \frac{1}{4} \left(2 \ln \frac{\Omega}{\omega_c} + 2\gamma_E \right) \left(\frac{\Omega}{\omega_c} \right)^2 + \mathcal{O}\left(\frac{\Omega}{\omega_c} \right)^3. \quad \text{(E12)}$$

Now

$$I_2(t) = \frac{e\Delta^2}{4\omega_c} \frac{\epsilon_0}{\Omega} \int_0^{\omega_c t} dx \frac{(3x - x^3)\sin \frac{\Omega}{\omega_c}x}{(1+x^2)^3}. \quad \text{(E13)}$$

As before, extend the upper limit to infinity,

$$I_2(t) = \frac{e\Delta^2}{4\omega_c} \frac{\epsilon_0}{\Omega} \int_0^{\infty} dx \frac{(3x - x^3)\sin \frac{\Omega}{\omega_c}x}{(1+x^2)^3}, \quad \text{(E14)}$$

and expanding this:

$$I_2(t) = \frac{e\Delta^2}{4\omega_c} \frac{\epsilon_0}{\Omega} \frac{\pi}{4} e^{-\Omega/\omega_c} \left[\left(\frac{\Omega}{\omega_c} \right)^2 + \mathcal{O}\left(\frac{\Omega}{\omega_c} \right)^4 \right]. \quad \text{(E15)}$$

Substituting Eqs. (E12) and (E15) into Eq. (E9), we obtain Eq. (29).

[1] C. Bäuerle, D. C. Glattli, T. Meunier, F. Portier, P. Roche, P. Roulleau, S. Takada, and X. Waintal, Rep. Prog. Phys. **81**, 056503 (2018).

[2] G. Wagner, D. X. Nguyen, D. L. Kovrizhin, and S. H. Simon, Phys. Rev. Lett. **122**, 127701 (2019).

[3] A. Furusaki and K. A. Matveev, Phys. Rev. Lett. **88**, 226404 (2002).

[4] U. Weiss, *Quantum Dissipative Systems*, Vol. 13 (World Scientific, Singapore, 2012).

[5] A. J. Leggett, S. Chakravarty, A. T. Dorsey, M. P. A. Fisher, A. Garg, and W. Zwerger, Rev. Mod. Phys. **59**, 1 (1987).

[6] P. P. Orth, A. Imambekov, and K. Le Hur, Phys. Rev. B **87**, 014305 (2013).

[7] K. Le Hur, in *Understanding Quantum Phase Transitions*, edited by L. D. Carr (Taylor and Francis, Boca Raton, 2010), Chap. 9.

[8] K. L. Hur, L. Henriet, L. Herviou, K. Plekhanov, A. Petrescu, T. Goren, M. Schiro, C. Mora, and P. P. Orth, Compt. Ren. Phys. **19**, 451 (2018).

[9] M. Sassetti and U. Weiss, Phys. Rev. Lett. **65**, 2262 (1990).

[10] R. Bulla, H.-J. Lee, N.-H. Tong, and M. Vojta, Phys. Rev. B **71**, 045122 (2005).

[11] K. Le Hur and M.-R. Li, Phys. Rev. B **72**, 073305 (2005).

[12] R. Schoelkopf, A. Clerk, S. Girvin, K. Lehnert, and M. Devoret, in *Quantum Noise in Mesoscopic Physics* (Springer, Berlin, 2003), pp. 175–203.

[13] Y. Makhlin, G. Schön, and A. Shnirman, in *New Directions in Mesoscopic Physics (Towards Nanoscience)* (Springer, Berlin, 2003), pp. 197–224.

[14] M. Grifoni, E. Paladino, and U. Weiss, Eur. Phys. J. B **10**, 719 (1999).

[15] L. Hartmann, I. Goychuk, M. Grifoni, and P. Hänggi, Phys. Rev. E **61**, R4687 (2000).

[16] P. Cedraschi and M. Buttiker, Ann. Phys. **289**, 1 (2001).

[17] F. B. Anders and A. Schiller, Phys. Rev. Lett. **95**, 196801 (2005).

[18] M. L. Wall, A. Safavi-Naini, and A. M. Rey, Phys. Rev. A **94**, 053637 (2016).

[19] A. Strathearn, P. Kirton, D. Kilda, J. Keeling, and B. W. Lovett, Nat. Commun. **9**, 3322 (2018).

[20] K. H. Yang, Y. Chen, H. Y. Wang, and B. Y. Liu, Phys. Lett. A **377**, 687 (2013).

[21] A. Galda, I. V. Yurkevich, and I. V. Lerner, Europhys. Lett. **93**, 17009 (2011).

[22] C. Rylands, N. Andrei, M. Goldstein, Y. Weiss, and R. Berkovits, Europhys. Lett. **86**, 67012 (2009).

[23] M. Goldstein, Y. Weiss, and R. Berkovits, Physica E **42**, 610 (2010).

[24] A. Komnik and A. O. Gogolin, Phys. Rev. B **68**, 235323 (2003).

[25] P. Wächter, V. Meden, and K. Schönhammer, Phys. Rev. B **76**, 125316 (2007).

[26] M. Goldstein, Y. Gefen, and R. Berkovits, Phys. Rev. B **83**, 245112 (2011).

[27] M. Goldstein and R. Berkovits, Phys. Rev. Lett. **104**, 106403 (2010).

[28] M. Goldstein and R. Berkovits, Phys. Rev. B. **82**, 235315 (2010).

[29] M. Goldstein and R. Berkovits, Phys. Rev. B **82**, 161307(R) (2010).

[30] G. A. Fiete, W. Bishara, and C. Nayak, Phys. Rev. B **82**, 035301 (2010).

[31] G. Yang, C.-H. Hsu, P. Stano, J. Klinovaja, and D. Loss, Phys. Rev. B **93**, 075301 (2016).

[32] L. Vannucci, F. Ronetti, D. Ferraro, J. Rech, T. Jonckheere, T. Martin, and M. Sassetti, J. Phys.: Conf. Series **969**, 012143 (2018).

[33] L. Vannucci, F. Ronetti, J. Rech, D. Ferraro, T. Jonckheere, T. Martin, and M. Sassetti, Phys. Rev. B **95**, 245415 (2017).

[34] D. Chevallier, J. Rech, T. Jonckheere, C. Wahl, and T. Martin, Phys. Rev. B **82**, 155318 (2010).

[35] F. Ronetti, L. Vannucci, D. Ferraro, T. Jonckheere, J. Rech, T. Martin, and M. Sassetti, Phys. Rev. B **98**, 075401 (2018).

[36] D. Litinski, P. W. Brouwer, and M. Filippone, Phys. Rev. B **96**, 085429 (2017).

[37] G. Fève, A. Mahé, J.-M. Berroir, T. Kontos, B. Placais, D. Glattli, A. Cavanna, B. Etienne, and Y. Jin, Science **316**, 1169 (2007).

[38] S. Hermelin, S. Takada, M. Yamamoto, S. Tarucha, A. D. Wieck, L. Saminadayar, C. Bäuerle, and T. Meunier, Nature **477**, 435 (2011).

[39] R. P. McNeil, M. Kataoka, C. J. Ford, C. H. Barnes, D. Anderson, G. A. Jones, I. Farrer, and D. A. Ritchie, Nature **477**, 439 (2011).

[40] J. Dubois, T. Jullien, F. Portier, P. Roche, A. Cavanna, Y. Jin, W. Wegscheider, P. Roulleau, and D. C. Glattli, Nature **502**, 659 (2013).

[41] E. Bocquillon, V. Freulon, F. D. Parmentier, J.-M. Berroir, B. Placais, C. Wahl, J. Rech, T. Jonckheere, T. Martin, C. Grenier, D. Ferraro, P. Degiovanni, and G. Fève, Ann. Phys. **526**, 1 (2014).

[42] C. Grenier, R. Hervé, G. Fève, and P. Degiovanni, Mod. Phys. Lett. B **25**, 1053 (2011).

[43] X.-G. Wen, Int. J. Mod. Phys. B **06**, 1711 (1992).

[44] J. von Delft and H. Schoeller, Ann. Phys. **7**, 225 (1998).

[45] D. Porras, F. Marquardt, J. von Delft, and J. I. Cirac, Phys. Rev. A **78**, 010101(R) (2008).

[46] A. Lemmer, C. Cormick, D. Tamascelli, T. Schaetz, S. F. Huelga, and M. B. Plenio, New J. Phys. **20**, 073002 (2018).

[47] J. Leppäkangas, J. Braumüller, M. Hauck, J.-M. Reiner, I. Schwenk, S. Zanker, L. Fritz, A. V. Ustinov, M. Weides, and M. Marthaler, Phys. Rev. A **97**, 052321 (2018).

[48] L. Magazzù, P. Forn-Díaz, R. Belyansky, J.-L. Orgiazzi, M. A. Yurtalan, M. R. Otto, A. Lupascu, C. M. Wilson, and M. Grifoni, Nat. Commun. **9**, 2298 (2018).

[49] R. P. Feynman and F. Vernon, Jr., Ann. Phys. **281**, 547 (2000).

[50] Our Hamiltonian differs from that in Ref. [14] by a minus sign in the definition of $\varepsilon(t)$ and $\Delta(t)$, hence the expressions below differ in the sign of $\Omega(t)$ from the results in that paper.

[51] M. Grifoni, M. Winterstetter, and U. Weiss, Phys. Rev. E **56**, 334 (1997).

[52] We did not consider the $\alpha = 1/2$ case in our previous work [2], since that paper was focused on the effect of Coulomb interactions on the current and these would renormalize α away from $1/2$ for an integer quantum Hall edge. Reference [2] studied the generalized master equation which is valid for $\alpha \ll 1$ and hence cannot be compared to the exact $\alpha = 1/2$ solution. On the other hand, in the present paper, we study the perturbative approach that can be benchmarked again the exact solution.

[53] K. Iwahori and N. Kawakami, Phys. Rev. A **94**, 063647 (2016).

[54] J. Keeling, A. V. Shytov, and L. S. Levitov, Phys. Rev. Lett. **101**, 196404 (2008).

[55] We always consider $\frac{a}{v}$ as our shortest timescale.

[56] V. S. Khrapai, A. A. Shashkin, M. G. Trokina, V. T. Dolgopolov, V. Pellegrini, F. Beltram, G. Biasiol, and L. Sorba, Phys. Rev. Lett. **99**, 086802 (2007).

[57] The term $\cos(2\alpha \arctan(v\tau/a))$ vanishes in this limit for $\alpha = \frac{1}{2\nu} = \frac{2n+1}{2}$..

[58] G. Fux, J. Keeling, and L. Brendon (private communication).

[59] M. Moskalets, G. Haack, and M. Büttiker, Phys. Rev. B **87**, 125429 (2013).

[60] It can be derived easily from Eq. (87) of Ref. [34].

[61] We explicitly set the chemical potential of the IQH edge to $\mu = 0$.

[62] The LHS is $\mathcal{O}(\epsilon)$ and thus can be neglected.

[63] The situation is much more complicated if the fermion $\hat{\psi}$ is neither chiral nor free.

[64] In this section, we omit all the (x, t) arguments for simplicity.